博 士 学 位 論 文

インターベンショナルラジオロジーにおける新規タングステン含有ゴムを使用した職業被ばくの低減

近 畿 大 学 大 学 院
医学研究科医学系専攻
木　嶋　健　太

Doctoral Dissertation

Reduction of the occupational exposure using a novel Tungsten-containing Rubber in Interventional Radiology

November 2019

Department of Medical Physics, Major in Medical Sciences
Kindai University Graduate School of Medical Sciences

Kenta Kijima

課博 ・ ~~論博~~

同　意　書

2019年 10月 15日

近畿大学大学院
医学研究科長　殿

共著者 Anchali ㊞　　共著者 田村 ㊞

共著者 ㊞　　共著者 西村恭昌 ㊞

共著者 ㊞　　共著者 ㊞

共著者 ㊞　　共著者 ㊞

共著者 ㊞　　共著者 ㊞

論文題目

Reduction of the occupational exposure using a novel Tungsten-containing Rubber in Interventional Radiology（インターベンショナルラジオロジーにおける新規タングステン含有ゴムを使用した職業被ばくの低減）

下記の学位論文提出者が、標記論文を貴学医学博士の学位論文（主論文）として使用することに同意いたします。

また、標記論文を再び学位論文として使用しないことを誓約いたします。

記

1．学位論文提出者氏名　　木嶋　健太

2．専攻分野　　医学系　　医学物理学

Reduction of the occupational exposure using a novel Tungsten-containing Rubber in Interventional Radiology

Kenta Kijima[1], Anchali Krisanachinda[2], Mikoto Tamura[1], Hajime Monzen[1], and Yasumasa Nishimura[3]

[1] Department of Medical Physics, Graduate School of Medical Sciences, Kindai University

[2] Department of Radiology, Faculty of Medicine, Chulalongkorn University

[3] Department of Radiation Oncology, Faculty of Medicine, Kindai University

ABSTRACT

This study aimed to investigate whether a novel tungsten-containing rubber (TCR) could be used to reduce the occupational exposure to operators against scattered radiation from a patient as substitute shielding material in interventional radiology (IR). The TCR is a lead-free radiation-shielding material that contains as much as 90% tungsten powder by weight. Air kerma rates of scattered radiation from solid-plate phantoms, simulating a patient, were measured with a semiconductor dosimeter at heights of the operator's eye (1600 mm from the floor), chest (1300 mm), waist (1000 mm), and knee (600 mm) with and without TCR shielding (1–5 mm thickness). The TCR and a commercial shielding material (RADPAD) were affixed onto the phantom on the operator's side and the reduction rates of the air kerma rate were compared. The reduction rates for TCR with thicknesses of 1, 2, 3, 4, and 5 mm at each height level were as follows; 70.37 ± 0.40%, 72.17 ± 0.29%, 72.95 ± 0.31%, 72.58 ± 0.35%, and 73.63 ± 0.63% at eye level; 76.36 ± 0.19%, 77.13 ± 0.10%, 77.36 ± 0.14%, 77.62 ± 0.25%, and 77.66 ± 0.14% at chest level; 67.78 ± 0.31%, 68.12 ± 0.19%, 68.88 ± 0.28%, 68.97 ± 0.14%, and 68.85 ± 0.45% at waist level; and 0.14 ± 0.94%, 0.72 ± 0.56%, 1.08 ± 0.74%, 1.77 ± 0.80%, and 1.79 ± 1.82% at knee level, respectively. The reduction rates with RADPAD were 61.80 ± 0.67%, 60.33 ± 0.61%, 64.70 ± 0.25%, and 0.14 ± 0.66% at eye, chest, waist, and knee levels, respectively. The shielding ability of the 1 mm TCR was superior to the RADPAD. The TCR could be employed to minimize an operator's radiation exposure instead of the commercial shielding material in IR.

Keywords : Radiation protection; Exposure, occupational; Exposure, personnel; Diagnostic radiology; Fluoroscopy

INTRODUCTION

Interventional radiology (IR) is a medical procedure where X-ray imaging is used to visualize the form or pathway of a blood vessel using contrast agents injected into the blood vessel through a catheter. IR is used for viewing the vessel under fluoroscopy. During IR procedures, there can be significant radiation exposure to not only the patient but also the medical staff because of the scattered radiation from a patient (Japanese Circulation Society Joint Working Group 2013). Although the medical staff wear radiation-protective aprons to protect the body (Sato et al. 2017), it cannot protect the head or limbs, therefore the dose to these parts for operators are increased over a period of time, which may increase their cancer risk (Shields et al. 2013). The International Commission on Radiation Protection has particularly recommended the reduction of dose limitations to protect the lens. With this background, identifying the source of the scattered radiation, considering the dose distribution, and developing effective shielding methods are expected to decrease radiation exposure in IR (*International Commission on Radiological Protection* 1996, 2000; Haga et al. 2017; Japanese Circulation Society Joint Working Group 2013; Sakamoto et al. 2009).

To overcome these problems, researchers have explored ways to provide effective X-ray protection using shielding materials (Sato et al. 2017) that was draped on the surface of the patient directly adjacent to the exposed area to significantly could reduce the radiation dose to the operator's hands and head (Schueler, 2010). To reduce the weight of such protection materials, several vendors have developed composite lead-equivalent materials using mixtures of various elements such as tin, copper, bismuth, antimony, and yttrium (Uthoff et al. 2014; Vlastra et al. 2017). These materials, however, may have harmful effects on the environment and possible toxicity if ingested. (DiPalma 2001; Agency for Toxic Substances and Disease Registry 2004, 2017; National Library of Medicine HSDB Database 2019)

Recently, the usefulness of tungsten functional paper (TFP), a flexible shielding material, was reported by Monzen et al. (Fujimoto et al. 2014; Kamomae et al. 2017; Monzen et al. 2017a, 2017b; Tamura et al. 2017). In a previous study, Dr. Monzen et al. showed that TFP had enough radiation shielding ability to protect against X-rays in the range of 60–120 kVp, and only one TFP sheet (thickness is 0.3 mm) could reduce scattered radiation from a water-equivalent slab phantom by >40% (Monzen et al. 2017b).

Tungsten-containing rubber (TCR) (Hayakawa Rubber Co., Ltd., Hiroshima, Japan), a novel shielding material that contains 90% tungsten powder by weight, was recently developed (Kijima et al. 2018; Kosaka et al. 2019). The TCR has superior waterproof and sterilization properties having reproducibility features compared to the TFP. Additionally, the TCR can be reused and is eco-friendly due to lead-free radiation shielding material. The purpose of this study was to investigate the utility of the TCR to reduce the operator's exposure against scattered X-ray radiation from the patient as a substitute for a commercial shielding material in IR. We evaluated the reduction rates of the air kerma rate at several body levels for an operator using various TCR thicknesses and compared the shielding ability of the TCR and a commercial shielding material.

MATERIALS AND METHODS

The radiation shielding abilities of the TCR and a commercial shielding material (RADPAD, Worldwide Innovations & Technologies, Inc., KS, USA) were compared by measurements of air kerma rate in IR. The nominal shielding efficiency of RADPAD with bismuth-antimony was 90% for 90 kVp X-ray (Chatterson et al. 2011). The elemental composition of TCR (mol%) was H: 1.0%, C: 6.5%, O: 0.5%, W: 90.0%, and others: 2% (Kijima et al. 2018). Table 1 shows the physical properties of TCR. The weight of 1 mm (thickness) × 250 mm (length) × 250 mm (width) for the TCR was 0.5 kg.

Table 1. Physical properties of tungsten-contained rubber

Item	Value	Standard
Thickness (mm)	1.0	JIS-K6250
Density (g/cm^3)	7.6	JIS-K6268
Hardness (Type-A)	77.0	JIS-K6253
Tensile strength (MPa)	4.5	JIS-K6251
Elongation (%)	400.0	JIS-K6251

Figure 1 shows the measurement geometry which had followed the previous study (Monzen et al. 2017b). A C-arm digital angiography system (Artis Zee; Siemens Healthineers, Erlangen-Forchheim, Germany) was employed, with the tube located underneath the table and a solid-plate phantom (SP33; IBA Dosimetry GmbH, Schwarzenbruck, Germany) was set on the table to simulate a patient. The solid-plate phantom was composed of polymethylmethacrylate with a density of 1.18 g/cm^3. Each solid-plate plane had dimensions of 300 mm (length) × 300 mm (width) × 10 mm (height), and total phantom thickness was 200 mm. The X-ray equipment had two modes: fluoroscopy mode and cine mode. The X-ray tube had added filtration of 0.8 mm of Al and 900 mm distance between the source and the detector. The field size was 27 inches (about 190 × 190 mm^2), and Table 2 shows the imaging parameters in this study. These values were measured with an area detector of an ionization chamber (DIAMENTOR chamber size B; PTW, Freiburg, Germany) automatically during IR.

A survey meter (semiconductor dosimeter, RaySafe X2 Survey sensor; Unfors RaySafe, Billdal, Sweden) was employed to measure the air kerma rate of scattered radiation from the phantom. This device is useful for measuring low-level radiation (dose range: 1 nGy – 9999 Gy), such as scattered radiation from X-ray tubes or in examination rooms.

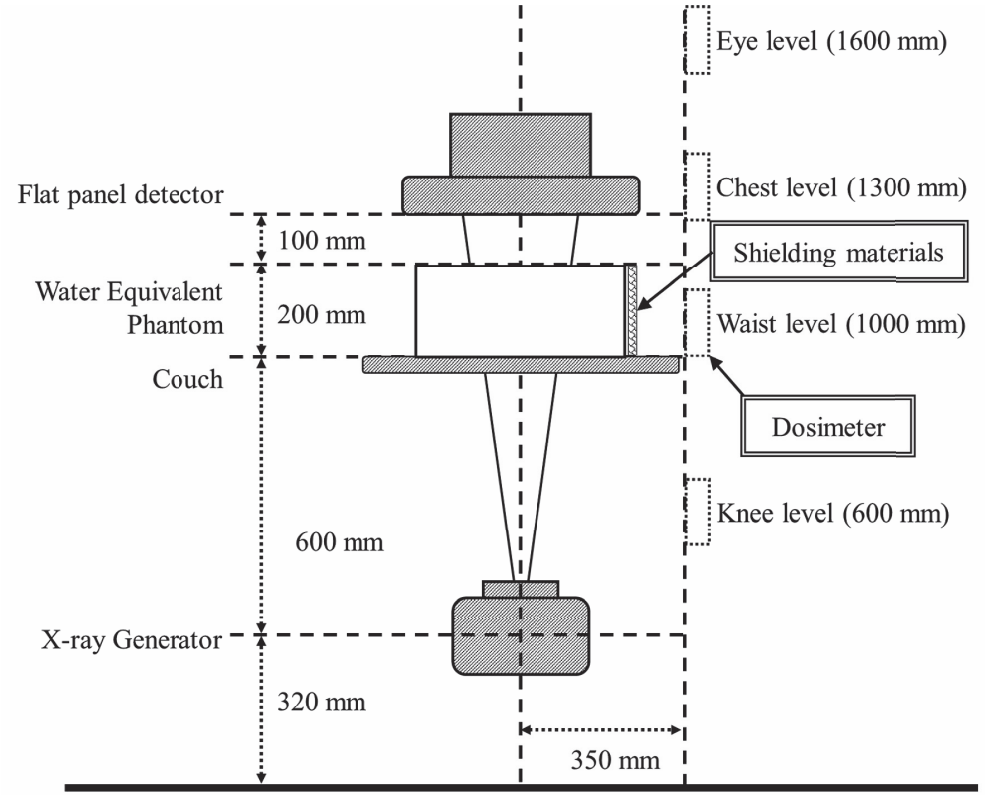

Figure 1. Experimental setup for detecting scattered radiation from a solid-plate phantom. The shielding material was taped to the operator side of the phantom. We then evaluated the shielding ability of tungsten-containing rubber (TCR) at various thicknesses including 0, 1, 2, 3, 4, and 5 mm.

Table 2. Imaging parameters of the C-arm digital angiography system

	Fluoroscopy	Cine
Pulse/frame rate (s^{-1})	15	7.5
Tube voltage (kV)	83.6	82.2
Tube current (mA)	232.3	231.2

Air kerma rates for the operator with TCR

The TCR was affixed onto the solid-plate phantom to the operator side, and the air kerma rate was measured with and without the TCR shielding. The thickness of the TCR rectangular sheets (200 × 250 mm) was increased from 1 to 5 mm in 1-mm increments.

We measured the air kerma rates at the height of the eyes (1600 mm from the floor), chest (1300 mm), waist (1000 mm) and knees (600 mm) of the operator in the both fluoroscopy mode and the cine mode, which were based on those determined in the previous study (Monzen et al. 2017b). Reduction rates were calculated from the following formula:

$$Reduction\ rate\ (\%) = \frac{Air\ kerma\ rate\ without\ TCR - Air\ kerma\ rate\ with\ TCR}{Air\ kerma\ rate\ without\ TCR} \times 100, \quad (1)$$

For all measurements, the semiconductor dosimeter detector faced the center of the solid-plate phantom to avoid the effect of angular dependence. Statistical errors were expressed as standard deviations estimated from three measurements at each height (Monzen et al. 2017b).

Comparison of reduction rate of the air kerma rate between TCR and RADPAD

The comparison of shielding efficiency between TCR and RADPAD was performed in fluoroscopy mode. The RADPAD was also set as shown in Figure 1 and the air kerma rate was measured with and without that the RADPAD in place. The upper edge of the solid-plate phantom and the end of the RADPAD were aligned at the measurement of eye and breast levels, and the lower edge of the solid-plate phantom and the end of the RADPAD were aligned at the measurement of waist and knee levels since the RADPAD (14.5 × 16.5 inch) was larger than the solid-plate phantom. The two-tailed unpaired Student's test was used to compare continuous variables and trends between the TCR and the RADPAD. The p-value < 0.05 was considered statistically significant.

RESULTS

Air kerma rates for the operator with TCR

The relative air kerma rates against scattered radiation by use of TCR with the thickness of 1-5 mm in 1 mm increments are shown in Table 3 and Figure 2. Additionally, the reduction rates of the air kerma rates are shown in Figure 3. Except at knee level, only 1 mm TCR reduced the air kerma rates >65%. The air kerma rates except at knee level were decreased up to 3.6% when the thickness of the TCR was increased from 2 mm to 5 mm. At knee level, even if the TCR thickness increased, there was very little reduction in the air kerma.

Table 3. Air kerma rates for various TCR thicknesses (1–5 mm)

	Fluoroscopy (μGy/min)					
TCR thickness	0 mm	1 mm	2 mm	3 mm	4 mm	5 mm
Eye level	6.0 ± 0.04	1.8 ± 0.01	1.7 ± 0.01	1.6 ± 0.01	1.7 ± 0.01	1.6 ± 0.03
Chest level	48.7 ± 0.09	11.5 ± 0.07	11.1 ± 0.03	11.0 ± 0.05	10.9 ± 0.09	10.9 ± 0.05
Waist level	134.9 ± 0.37	43.5 ± 0.69	43.0 ± 0.03	42.0 ± 0.05	41.9 ± 0.09	42.0 ± 0.05
Knee level	194.2 ± 0.99	193.9 ± 1.54	192.8 ± 0.43	192.1 ± 1.02	190.8 ± 1.17	190.7 ± 3.33

TCR = tungsten-contained rubber.

	Cine (μGy/min)					
TCR thickness	0 mm	1 mm	2 mm	3 mm	4 mm	5 mm
Eye level	129.0 ± 2.95	51.5 ± 1.33	49.3 ± 1.12	48.5 ± 1.12	48.4 ± 1.20	46.8 ± 0.79
Chest level	1344.5 ± 16.66	311.0 ± 9.45	303.6 ± 7.61	296.9 ± 5.19	294.8 ± 9.74	293.7 ± 6.05
Waist level	3544.3 ± 2.05	1500.0 ± 9.27	1489.7 ± 17.93	1465.7 ± 16.50	1454.3 ± 26.40	1453.7 ± 24.58
Knee level	6683.7 ± 12.12	6597.0 ± 6.38	6592.7 ± 16.03	6606.0 ± 7.26	6664.7 ± 5.00	6615.0 ± 5.10

TCR = tungsten-contained rubber.

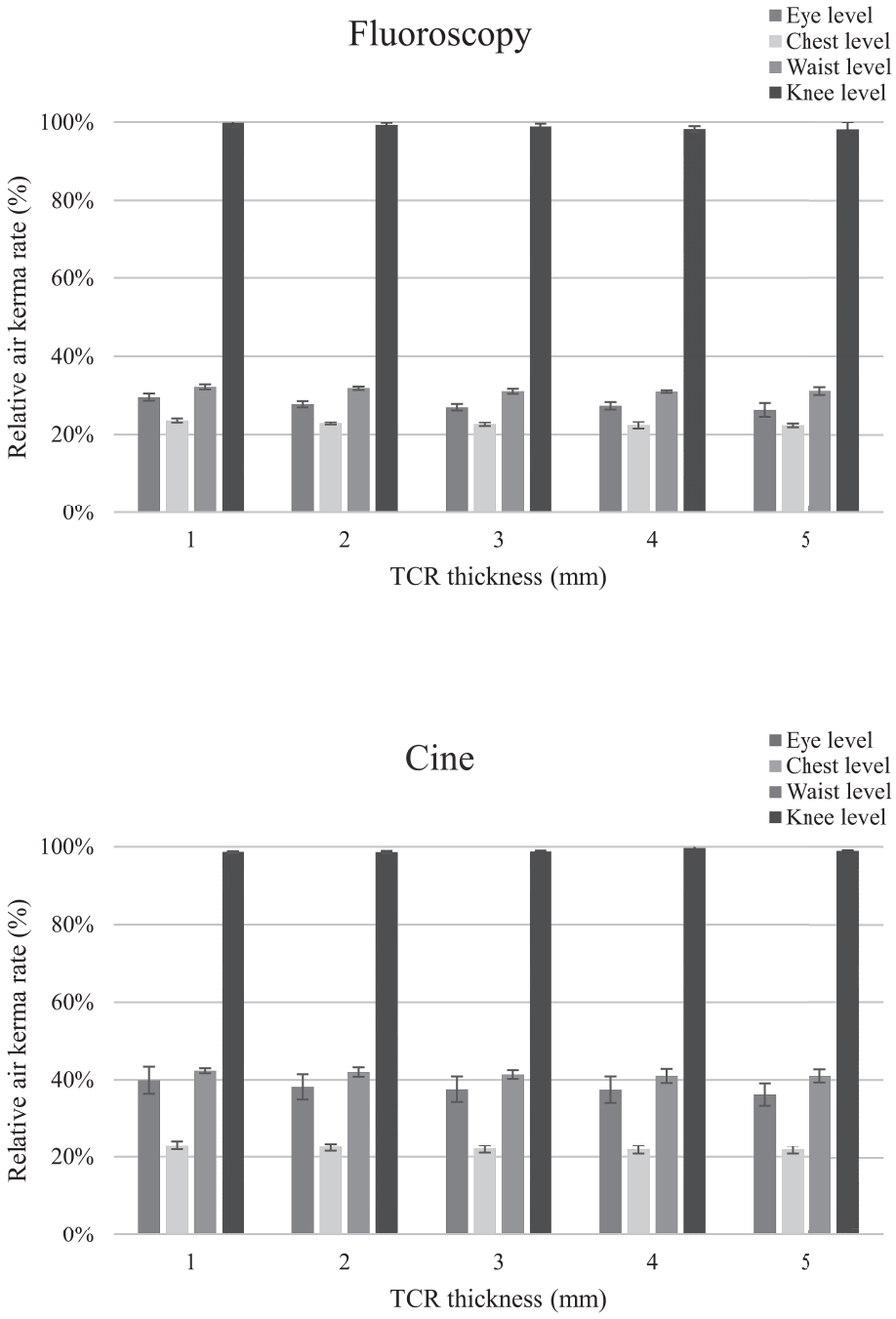

Figure 2. Relationships between each TCR thickness and the relative air kerma rate for each height (body) level. The relative air kerma rates were normalized by the air kerma rates without TCR for each height.

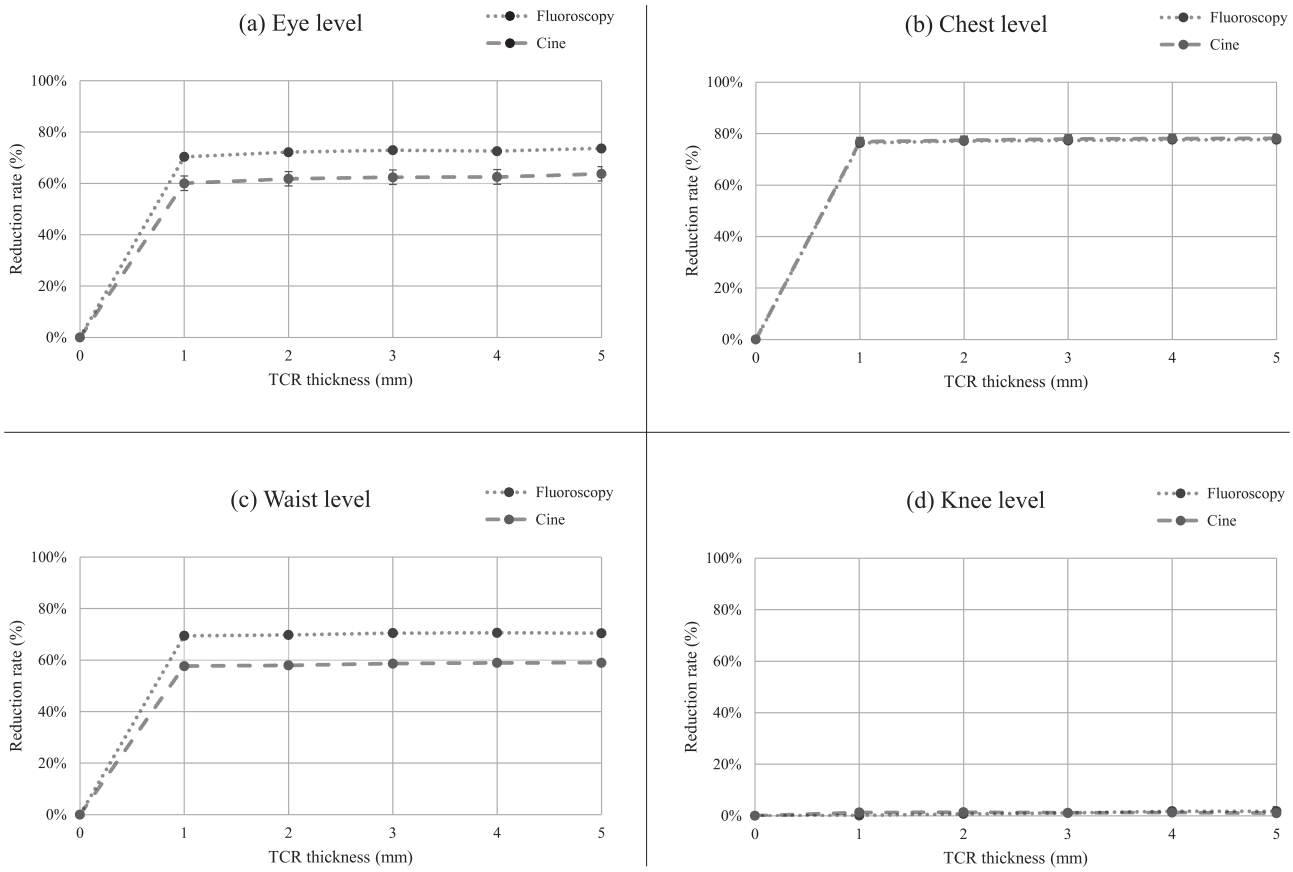

Figure 3. Relationships between each TCR thickness and the reduction rate for each height (body) level. The reduction rate was normalized according to the measurement value without TCR for each TCR thickness.

Comparison of reduction rate of the air kerma rate between TCR and RADPAD

The comparison of reduction rate between TCR and RADPAD against scattered radiation in fluoroscopy mode are shown in Table 4. Except at knee level, reduction rates of TCR were significantly ($p < 0.01$) lower than that of RADPAD.

Table 4. Reduction rates for 1 mm TCR and RADPAD at each height (body) level in fluoroscopy mode

Materials	1 mm TCR	RADPAD
Eye level	70.37 ± 0.40%	61.80 ± 0.67%
Chest level	76.36 ± 0.19%	60.33 ± 0.61%
Waist level	67.78 ± 0.33%	64.70 ± 0.25%
Knee level	0.14 ± 0.60%	0.07 ± 0.66%

TCR = tungsten-contained rubber. The reduction rates were normalized according to the measurement value without shielding material of corresponding height level.

DISCUSSION

The shielding ability of the TCR was investigated to protect against scattered radiation from a patient in IR. The reduction rates of the air kerma at eye, chest, and waist were approximately 65–70% for 1 mm TCR. Additionally, the air kerma rates were reduced only up to 3.6% with additional layers of TCR, which indicated 1 mm TCR exhibited saturated shielding ability to protect against scattered radiation in IR. The direct scattered radiation to the TCR was enough to be shielded by the 1 mm TCR. The result of reduction rates of the air kerma at knee shows the TCR affixed to the patient's side does not contribute to the attenuation of knee-level radiation since the radiation dose at the knee comes directly from the x-ray tube and the scatter from the table (Monzen et al. 2017b). With comparing to result of previous study (Monzen et al. 2017b), 1 mm TCR adequately reduces the radiation exposure by scattered radiation from a patient. However, a TCR with a thickness of <1 mm may not provide enough tensile strength and tear resistance so it may not be reusable, especially after the heat or gas sterilization.

The shielding efficiency of 1 mm TCR was 9 to 16% greater than RADPAD at the eye and chest levels. Additionally, the TCR can be reused and is eco-friendly, while the RADPAD is disposable and not as friendly to the environment compared to the TCR due to the inherent bismuth and antimony. Therefore, the TCR was could be used in clinical practice with further development. The TCR had waterproof and sterilization capabilities, that could be an advantage around the over TFP (Monzen et al. 2017b). The price of the TCR was approximately five times than that of RADPAD. However, the TCR can be reused, resulting in better cost performance and making it more eco-friendly than RADPAD.

To protect the eye, chest, waist, arms, and hands of operators from scattered radiation, TCR affixed to a patient side could be useful. On the other hand, to get reduction at the knee, a couch curtain or shielding panel is need. Therefore, to protect the whole body of operators from scattered radiation, it is important to use the combination of the TCR affixed to patient's side and common personal protective devices such as a couch curtain and shielding panel (Duran et al. 2013; Haga et al. 2017; Sato et al. 2017). The TCR may be more flexible for operators to prevent radiation exposure since the TCR is easy to cut, fold, and affix to the other materials and is lead-free, reusable, and waterproof, as compared to typical commercial shielding material in IR.

CONCLUSION

The 1 mm thickness of TCR has adequate radiation-shielding ability to reduce the operator's radiation exposure against scattered radiation from patients in a typical IR procedure.

ACKNOWLEDGMENTS

The authors thank Unfors RaySafe in Thailand for technical assistance and for providing the semiconductor dosimeter RaySafe X2. We also thank Dr. Petchaleya Suwanpradit and the staffs of the Division of

Interventional Radiology, King Chulalongkorn Memorial Hospital for providing suitable equipment to validate the application of TCR as described in this manuscript. This work was supported partly by JSPS KAKENHI grant numbers 16K09027 and 17K09071.

REFERENCES

1. Agency for Toxic Substances and Disease Registry. Toxicological profile for Copper [online], Atlanta, GA:US Department of Health and Human Services, Public Health Service;2004. Available at https://www.atsdr.cdc.gov/toxprofiles/tp.asp?id=206&tid=37. Accessed 16 March 2019.
2. Agency for Toxic Substances and Disease Registry. Toxicological profile for Antimony and Compounds [online], Atlanta, GA:US Department of Health and Human Services, Public Health Service;2017. Available at https://www.atsdr.cdc.gov/toxprofiles/tp.asp?id=332&tid=58. Accessed 16 March 2019.
3. Chatterson LC, Leswick DA, Fladeland DA, Hunt MM, Webster ST. Lead versus Bismuth-Antimony Shield for Fetal Dose Reduction at Different Gestational Ages at CT Pulmonary Angiography. Radiology 260:560–567;2011. Doi:10.1148/radiol.11101575.
4. DiPalma JR. Bismuth Toxicity, Often Mild, Can Result in Severe Poisonings Emerg Med News 23:16;2001. Doi:10.1097/00132981-200104000-00012.
5. Duran A, Hian SK, Miller DL, Le Heron J, Padovani R, Vano E. Recommendations for occupational radiation protection in interventional cardiology. Catheter Cardiovasc Interv 82, 29–42;2013. Doi:10.1002/ccd.24694.
6. Fujimoto T, Monzen H, Nakata M, Okada T, Yano S, Takakura T, Kuwahara J, Sasaki M, Higashimura K, Hiraoka M. Dosimetric shield evaluation with tungsten sheet in 4, 6, and 9MeV electron beams. Phys Medica 30, 838–842;2014. Doi:10.1016/j.ejmp.2014.05.009.
7. Haga Y, Chida K, Kaga Y, Sota M, Meguro T, Zuguchi M. Occupational eye dose in interventional cardiology procedures. Sci Rep 7, 1–7;2017. Doi:10.1038/s41598-017-00556-3.
8. International Commission on Radiological Protection. Avoidance of Radiation Injuries from Medical Interventional Procedures. Oxford:Pergamon Press;ICRP Publication 85;2000.
9. International Commission on Radiological Protection. Radiological Protection and Safety in Medicine. Oxford:Pergamon Press;ICRP Publication 73;1996.
10. Japanese Circulation Society Joint Working Group. Guideline for Radiation Safety in Interventional Cardiology (JCS 2011). Circ J 77, 519–549;2013. Doi:10.1253/circj.CJ-66-0056.
11. Kamomae T, Monzen H, Kawamura M, Okudaira K, Nakaya T, Mukoyama T, Miyake Y, Ishihara Y, Itoh Y, Naganawa S. Dosimetric feasibility of using tungsten-based functional paper for flexible chest wall protectors in intraoperative electron radiotherapy for breast cancer. Phys Med Biol 63, 015006;2017. Doi:10.1088/1361-6560/aa96cf.
12. Kijima K, Monzen H, Matsumoto K, Tamura M, Nishimura Y. The Shielding Ability of Novel Tungsten Rubber Against the Electron Beam for Clinical Use in Radiation Therapy. Anticancer Res 38, 3919–3927;2018. Doi:10.21873/anticanres.12677.

13. Kosaka H, Monzen H, Matsumoto K, Tamura M, Nishimura Y. Reduction of Operator Hand Exposure in Interventional Radiology with a Novel Finger Sack Using Tungsten-Containing Rubber. Health Phys 1;2019. Doi:10.1097/HP.0000000000000992.
14. Monzen H, Kanno I, Fujimoto T, Hiraoka M. Estimation of the shielding ability of a tungsten functional paper for diagnostic x-rays and gamma rays. J Appl Clin Med Phys 18, 325–329;2017a. Doi:10.1002/acm2.12122.
15. Monzen H, Tamura M, Shimomura K, Onishi Y, Nakayama S, Fujimoto T, Matsumoto K, Hanaoka K, Kamomae T. A novel radiation protection device based on tungsten functional paper for application in interventional radiology. J Appl Clin Med Phys 18, 215–220;2017b. Doi:10.1002/acm2.12083.
16. National Library of Medicine HSDB Database, Yttrium [online], Bethesda, MD US. U.S. National Library of Medicine;2019. Available at https://pubchem.ncbi.nlm.nih.gov/compound/yttrium#section=Hazards-Identification Accessed 16 March 2019.
17. Sakamoto H, Ikegawa H, Kobayashi H, Kiuchi T, Sano Y, Fukasawa M, Araki T. A study of operator's hand and finger exposure dose reduction during angiographic procedures. Nihon Hoshasen Gijutsu Gakkai Zasshi 65, 25–34;2009. Doi:10.6009/jjrt.65.25.
18. Sato N, Fujibuchi T, Toyoda T, Ishida T, Ohura H, Miyajima R, Orita S, Sueyoshi T. Consideration of the Protection Curtain's Shielding Ability after Identifying the Source of Scattered Radiation in the Angiography. Radiat Prot Dosimetry 175, 238–245;2017. Doi:10.1093/rpd/ncw291.
19. Schueler BA. Operator Shielding:How and Why. Tech Vasc Interv Radiol 13, 167–171;2010. Doi:10.1053/j.tvir.2010.03.005.
20. Shields LB, Coons JM, Dedich C, Ragains M, Scalf K, Vitaz TW, Spalding AC. Improvement of therapeutic index for brain tumors with daily image guidance. Radiat Oncol 8, 283;2013. Doi:10.1186/1748-717X-8-283.
21. Tamura M, Monzen H, Kubo K, Hirata M, Nishimura Y. Feasibility of tungsten functional paper in electron grid therapy:a Monte Carlo study. Phys Med Biol 62, 878–889;2017. Doi:10.1088/1361-6560/62/3/878.
22. Uthoff H, Benenati MJ, Katzen BT, Pena C, Gandhi R, Staub D, Schernthaner M. Lightweight Bilayer Barium Sulfate–Bismuth Oxide Composite Thyroid Collars for Superior Radiation Protection in Fluoroscopy-guided Interventions:A Prospective Randomized Controlled Trial. Radiology 270, 601–606;2014. Doi:10.1148/radiol.13122834.
23. Vlastra W, Delewi R, Sjauw KD, Beijk MA, Claessen BE, Streekstra GJ, Bekker RJ, van Hattum JC, Wykrzykowska JJ, Vis MM, Koch KT, de Winter RJ, Piek JJ, Henriques JPS. Efficacy of the RADPAD Protection Drape in Reducing Operators' Radiation Exposure in the Catheterization Laboratory. Circ Cardiovasc Interv 10, e006058;2017. Doi:10.1161/CIRCINTERVENTIONS.117.006058.